

Plasma drift motion in the F-region of the ionosphere using photometric nightglow measurements

G K Mukherjee

Indian Institute of Geomagnetism, New Panvel(W), Navi Mumbai 410 218 (MS), India

e-mail: gkm@iigs.iigm.res.in

and

D J Shetti

Department of Physics, Shivaji University, Kolhapur 416 004 (MS), India

Received 12 February 2007; revised 26 July 2007, accepted 7 January 2008

The equatorial ionospheric plasma irregularities have been studied in the last few years by different ground based (radar, digisonde, GPS, optical instruments) techniques and *in situ* rocket and satellite measurements. The time evolution and propagation characteristics of these irregularities have been used to study the important aspects of ionospheric dynamics and thermosphere-ionosphere coupling. In this study the plasma drift motion has been inferred in zonal and meridional directions at Kolhapur (16.8°E, 74.2°E, dip latitude 10.6°N) by measuring the OI 630.0 nm intensities at three directions in zenith using tilting filter photometers. Also, the observed zonal plasma drift velocities are compared with the thermospheric zonal neutral wind velocities obtained from the HWM-93 model to investigate the thermosphere-ionosphere coupling. In general there is good agreement between the model predictions and the observations. The HWM-93 model also reproduces well the altitudinal and latitudinal variations of the neutral wind velocity in the low latitude region. The dominant periodicities observed in OI 630.0 nm intensity fluctuations on a Spread-F night were typically varying between 30 and 50 min.

Keywords: Ionospheric irregularities, Plasma irregularities, F-region ionosphere, Nightglow, Photometric nightglow

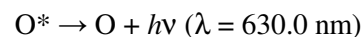
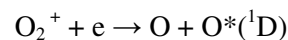
PACS No.: 94.20.Ac

1 Introduction

The equatorial ionospheric irregularities associated with night time equatorial spread-F phenomena have been observed using ionosondes, topside sounders, and *in situ* rocket and satellite measurements as well as optical techniques (conventional tilting and scanning photometers and wide angle optical imaging systems)¹⁻⁵. The continuing interest in the studies related to the equatorial spread-F irregularities increased from its implications for trans-ionospheric communications and navigation systems.

The scale size of the irregularities varies between tens of centimeters to hundreds of kilometers, which are very sensitive to a wide range of diagnostic techniques. Several research workers^{1,2} have used wide angle imaging of F-region night glow emissions to study large scale plasma irregularities. The irregularities characterized by large scale ionospheric plasma depletions are generally called plasma bubbles. These are the regions where the plasma densities decrease abruptly by several orders of magnitude compared to the ambient plasma densities.

The nightglow emission of OI 630 nm is produced at the bottom side of the ionospheric F-region, at about 250-300 km altitude, by the dissociative recombination process³ and commonly used to investigate the thermospheric/ionospheric processes at F-region heights at night. There are other processes, like photo-dissociation and photo-electron excitation contributing to O¹D state of OI 630.0 nm emission. Mainly nightglow of OI 630.0 nm emission due to dissociative recombination process is discussed here.



Equatorial F-region irregularity studies using a monochromatic (OI 630.0 nm emission) all-sky imaging photometer system were first conducted by Weber *et al.*² These observations showed the first images of magnetically quasi-N-S aligned structures of low intensity OI 630.0 nm emission with east-west scale sizes ranging from 40 to 450 km usually drifting eastward and the plasma bubble drift velocities were

fairly close to the zonal ambient plasma drift velocities during the period of spread-F observations. These low-intensity regions are the optical signatures of depletions, which are mapped in the all-sky images of OI 630.0, 577.7 and 777.4 nm emissions. According to present theoretical interpretations, large scale plasma depletions or spread-F bubbles are initially generated at the F-region bottom side, through a fluid type gradient instability mechanism, such as the gravitational Rayleigh-Taylor instability in conjunction with $\mathbf{E} \times \mathbf{B}$ instability with seeding perturbations provided by gravity waves, vertical winds and electric fields, etc. Evidence from backscatter radar⁶ shows, that quasi-periodic bubbles or Equatorial Spread-F (ESF) could be seeded by gravity waves, having horizontal wavelengths of the order of 100 km at altitudes of around 200 km (the bottom of the F-Layer).

The ionospheric plasma bubbles (depletions) are generally aligned along the magnetic field lines, owing to their much greater conductivity in the magnetic field direction as compared with the perpendicular conductivity. As these bubbles move buoyantly upward with respect to the ambient plasma in the equatorial region, their bottom side feet migrate away from the equator, reaching dip latitudes of over $\pm 15^\circ$. At the boundaries and within the bubbles, small scale size irregularities are generally produced, which give rise strong VHF nighttime scintillations in satellite beacon signals. The plasma drift velocities associated with the bubbles constitute an important parameter for thermospheric studies. These bubbles usually drift eastward in the equatorial ionosphere and are often tilted to the west of the magnetic meridian because of the bubble upward motion. In this paper the authors present and discuss some of the results of the ionospheric plasma movements (zonal and meridional drifts) from the OI 630.0 nm photometric measurement carried out at Kolhapur on Spread-F nights. A comparison of the observed component of the plasma (ambient and depletion) drift velocity with component of F-region neutral wind from a model⁷ has also been made.

2 Tilting-filter photometers

The observations were made using a set of three tilting-filter photometers³. The photometers have a one degree field of view (overall) giving a cross-section of about 5 km in the F-region height (250 km) when looking at zenith. The interference filter (Barr Associates, USA) when kept at a temperature of 23°C has a pass-band centered at about 630 nm for

normally incident light. The bandwidths of the filters are about 1 nm with 60 % transparency. The airglow intensity is determined from the difference of the background with signal and backgrounds only. The photometers are quite portable and can easily be mounted to point towards any desired combination of zenith and azimuth angles. Here horizontal motions in the thermosphere can be measured by pointing the photometers in three different directions. Typically one of the photometers is pointed to zenith, second one to the north/ south and third photometer is directed to the east or west.

3 Results and discussion

In Fig. 1 are plotted the nocturnal variation of OI 630.0 nm emission at zenith angle 30°E and 30°W at Kolhapur on 18-19 Feb. 1991. These represent the local zenith intensities at about 144.5 km east and west of Kolhapur, if the emission height is assumed to be 250 km. It was a magnetically quiet night with $A_p = 4$. The large dips in intensities, which are the optical signature of moving ionospheric plasma bubbles marked in the diagram as A and B in two plots. The movement of airglow structures from west (A, B) to

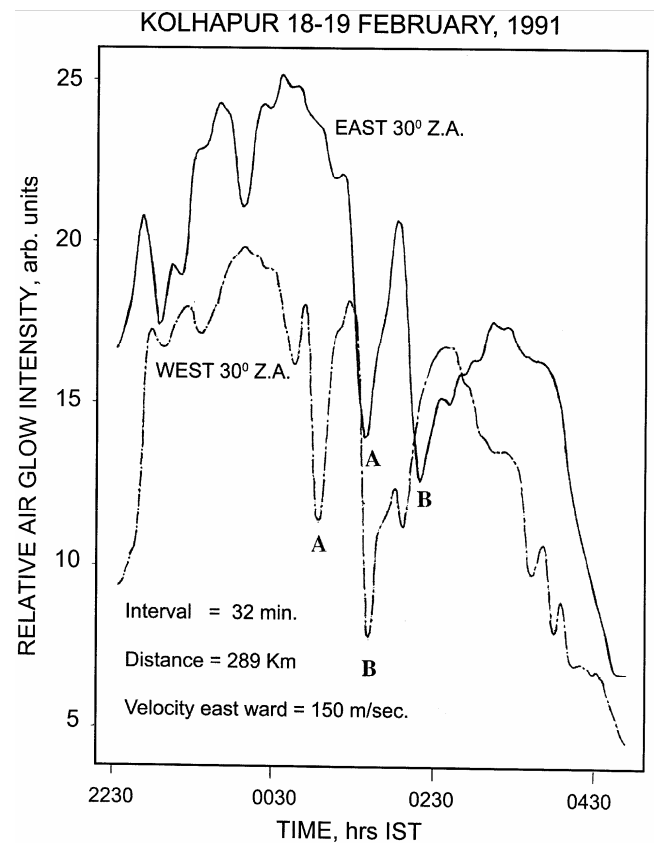


Fig. 1 — Plot of nocturnal variation of OI630.0 nm intensity as a function of time (IST) on 18-19 Feb. 1991 at Kolhapur

east (A, B) is obvious, however, sometimes the structures change considerably as they move, making it more difficult to track common features and hence determine the motion. These difficulties can be overcome by reducing the spacing between the regions being observed in the F-region.

The authors also determine the apparent drift speeds simply from the time delay of common features (maxima or minima) in the data which gave zonal drifts as 150 m/s. It has been tacitly assumed that the maxima progress at a constant speed and at a constant height of 250 km, the shape remaining unchanged. The local time difference, though small, between the E and W observations has no bearing on the interpretation. The source of error in this type of calculation can arise due to change in the constant height (250 km) of the layer assumed in the computation. A change of ± 10 km in assumed vertical height in the F-region during the movement of the bubble can give rise to an error of ± 5 m/s in computations of drift speeds. Another source of error could be due to inaccurate estimate of the time of occurrence at which airglow fluctuations reach their maxima or minima. As the airglow data used were having sampling rate of 2 min, error due to inaccuracy of such time scale in the determination of velocity would be about ± 10 m/s. Few more examples of thermospheric motion in eastward direction and north-south directions are also provided, as shown in Figs 2, 3 and 4 for the three nights. In Fig. 5 the propagating wavy disturbances are depicted in OI 630.0 nm in all three zenith angles on a typical spread-F night. The VHF scintillation recording at Kolhapur also showed moderate to strong scintillation activity present in the received radio beacon signal (at 250 MHz) from FLEETSAT satellite on all these nights. The rate of change of meridional wind ($\Delta U/\Delta t$) at night varies with pressure gradient term, $(1/\rho) \Delta p/\Delta y$, ion-drag and viscosity terms in the momentum equation⁸. A rough estimate of the effect of these may be obtained from the average value of observed change in drift velocity during the night. Figure 1 also shows depletions in airglow intensity with larger depths (deepened minima at 0100 hrs IST was about 40 %). Durations of the depletions vary between 10 and 20 min, which is of the order of the growth period of a typical equatorial ionospheric plasma bubble⁹.

It is worth noting that instead of taking times of minima for computation of velocity if one chooses the time difference of maxima, it results into the same numerical value of drift velocity. This shows that

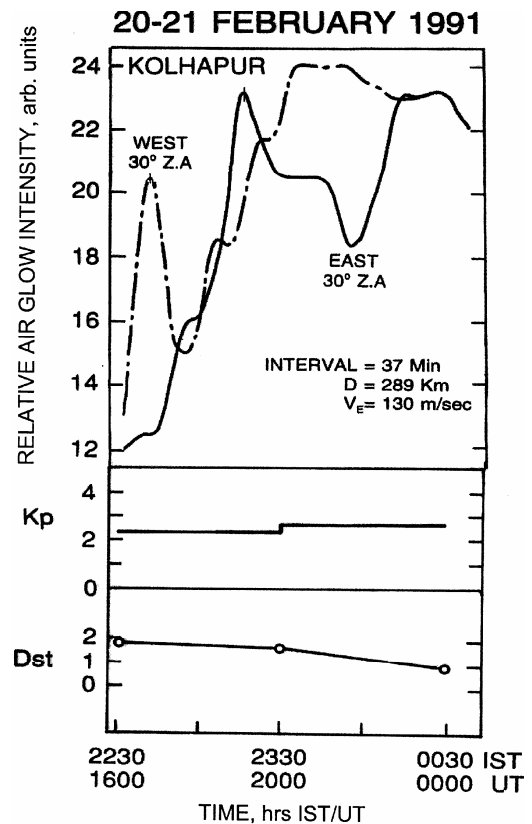


Fig. 2 — Plot of variation of OI 630.0 nm intensity as a function of time (IST) on 20-21 Feb. 1991 at Kolhapur

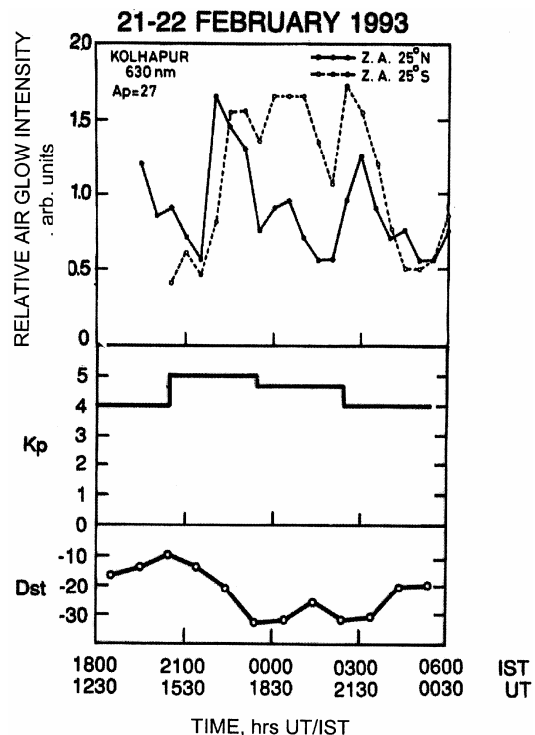


Fig. 3 — Plot of variation of OI 630.0 nm intensity as a function of time (IST) on 21-22 Feb. 1993 at Kolhapur

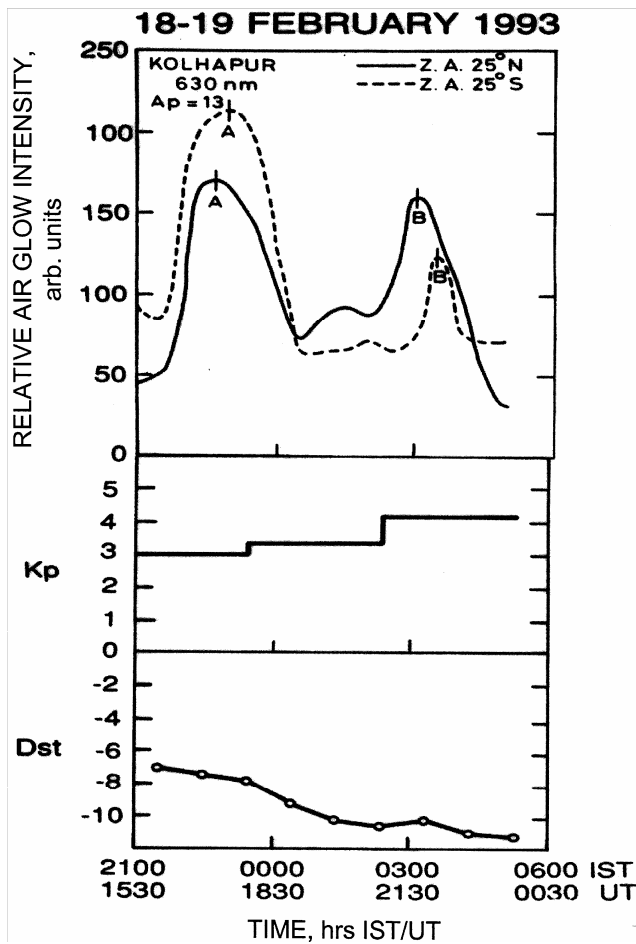


Fig. 4 — Plot of variation of OI 630 nm intensity at 25N and 25S direction as a function of time (hrs IST) on 18-19 Feb. 1993 at Kolhapur

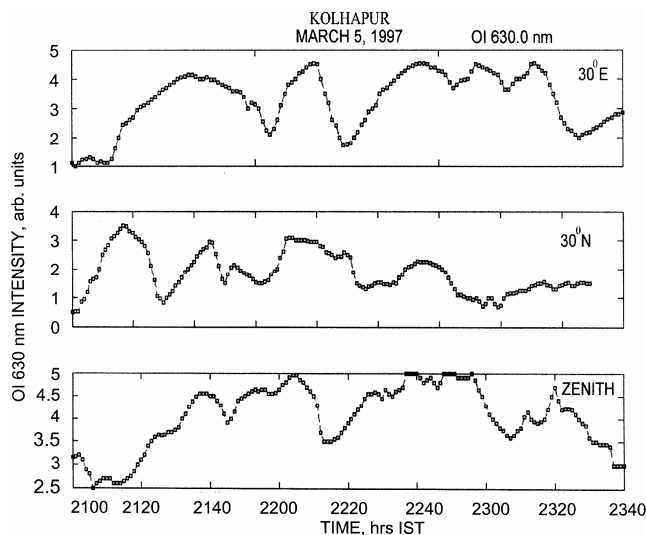


Fig. 5 — Variation of OI 630.0 nm intensity along 30°E, 30°N and zenith directions on the night of 5 Mar. 1997 at Kolhapur showing propagating wavy disturbances on a Spread-F night

Table 1 — Results of spectral power (in arb. units) of the fluctuations in OI 630.0 nm on 18-19 Feb. 1991

Band	2230-0038 IST		0038-0246 IST	
	East 30°Z.A	West 30° Z.A	East 30° Z.A.	West 30°Z.A
4-15 min	19.88	11.02	20.76	165.0
15-30 min	70.08	20.20	352.00	966.4
30 min-1 h	429.80	22.60	1549.20	2157.4
Spectral slope	- 3.23	- 2.63	- 4.24	- 5.13

airglow depletions move with the same velocity as background plasma. That is how the drift motions of the bubbles have been suggested to trace the motion of ambient plasma¹⁰ at low latitudes. It may be noted from Fig. 1 that during 0130-0330 hrs IST strong VHF scintillation activity was also recorded at Kolhapur (not shown in Fig. 1). Rastogi and Aaron⁴ have shown that geomagnetic activity has a strong effect on the occurrence of range type spread-F and scintillation. The occurrence of scintillations during post-midnight hours was shown to be greatly enhanced during internationally disturbed days.

In comparison with international quiet days, especially during low sunspot years, they also showed that besides the usual pre-midnight events, any abnormal reversal of the equatorial horizontal electric field (normally westward at night) to the eastward direction at night is followed by occurrence of intense VHF scintillation with delay time of one hour.

In Table 1, the results of power spectra of the fluctuations in OI 630.0 nm are presented on 18-19 Feb. 1991 (Fig. 1). Total power integrated over the three bands (4-15 min; 15-30 min, 30 min-1 h) obtained by two photometers, looking at east and west directions with zenith angle of 30° have been computed, thereby restricting airglow fluctuations relatively to longer periods. The spectral analysis was conducted by means of the fast Fourier Transform (FFT) method using 64 point data at an interval of 2 min tapered by 4JI prolate window¹¹. It is clearly seen that during 2230 to 0038 hrs IST, the power is higher in all three bands for airglow fluctuations seen by photometer pointing to the eastern sky, as compared to the westward looking photometer. On the contrary, during 0038 to 0246 hrs IST, west photometer portrays more fluctuations in three bands compared to corresponding observed fluctuations in the eastern sky. Also eastward propagating disturbances are noticed (Fig. 1). This implies that as the airglow structures move towards east, their intensities decrease and fluctuations diminish during

the post-midnight hours. This could also be attributed to the vertical movement of the F-layer during its propagation from west to east. Similarly, the typical spectral indices show higher values in three bands for west photometer data compared to the east photometer record during the same interval.

It is worth noting that the spectra are clearly dominated by long period waves. The airglow intensities within the depletions were typically 40% of the background levels. The scale size of the structure is about 150 km. It can be shown that horizontal wavelength of the irregularities smaller than twice the diameter of the field of view will be strongly attenuated. If the diameter of the field of view is 5 km (assuming height of maximum OI 630.0 nm emission as 250 km), horizontal wavelength shorter than 10 km is strongly attenuated¹². For a horizontal drift velocity of 150 m/s, this will correspond to frequencies greater than 15×10^{-3} Hz. The spectra are dominated by longer period waves.

In Fig. 2, the plot of variation OI 630.0 nm intensity is shown, as seen by two tilting photometers looking at 30°E and 30°W directions from Zenith. Also, the magnetic activity index Kp and Dst values in the lower two panels are plotted, to know the condition of geomagnetic activity during the period of observations. As it is evident, it was a magnetically quiet night. The large dips in OI 630.0 nm intensity around 2250 and 2350 hrs IST are the optical signature of eastward propagating ionospheric plasma bubbles, as observed by the two photometers. The speed of the bubble is considerably reduced to 80 m/s during its movement from west to eastward direction.

Figure 3 shows the typical airglow (OI 630.0 nm) variations on a magnetically disturbed night ($A_p = 27$) at Kolhapur. The highest Kp index during the night was 5 with A_p value for the day as 27. It is clearly seen that wave of period of 3-4 h is present both in Dst and airglow data (OI 630.0 nm). The observed ionospheric height variations (both positive and negative effect) at low latitudes during magnetic storms are dependent on factors like changes in dynamics, heating and composition of the ionosphere, which take place depending upon latitude, longitude, local time and phase of the geomagnetic storm¹³. The electron concentration at low latitude may vary drastically during magnetic storms. The perturbation of $\pm 50\%$ from the quiet time densities is usually enhanced at low latitudes during geomagnetic disturbances, while the height of the F-layer typically fluctuates a few tens of kilometers. During severe

magnetic storms, however, decreases in electron density may occur at all latitudes depending on the local time.

Rishbeth *et al.*¹³ reported that in general, the equatorial anomaly is less developed during storm periods. However, there are cases when the enhancements are strongly manifested in the crest region and critical frequency in the equatorial trough is reduced compared to quiet days. Takahashi *et al.*¹⁴ have reported ionization enhancements at low latitudes during disturbed conditions. They showed that these enhancements were having an equatorial anomaly-like structure having a minimum at the dip equator. Fesen *et al.*¹⁵ reported the prominent enhancement of F-region critical frequency in the ionization crest region during disturbed days. Sahai *et al.*¹⁶ also compared the variations of F-region parameters (f_oF2 and $h'F$) with ground based observations of [OI] 777.4 nm, OI 630.0 nm and 557.7 nm from Cachoeira Paulista (22.7°S, 38.4°W), Brazil, an equatorial station, during magnetic disturbances. They found that the dynamical variations in the F-region ionosphere are correlated with the non-diurnal variations observed in the atomic oxygen airglow emissions at both equatorial and low latitudes¹⁶.

In Fig. 4, one more example of thermospheric motion in meridional direction using OI 630.0 nm intensity variations at 25°N and 25°S directions is presented and discussed. The wave activity is apparently not observed on this night perhaps due to smoothing of the data. It is noted that the drift speed (175 m/s) is in equator ward (N-S) direction during the first half of the night (2300 hrs IST) and also around 0300 hrs IST, signifying the steady flow of the meridional component of the neutral wind during the night.

Figure 5 shows the variation of OI 630.0 nm intensity along 30°E, 30°N and Zenith directions on the night of 5 Mar. 1997 at Kolhapur showing propagating wavy disturbances on a Spread-F night. Figure 5 presents a typical recording of the propagating airglow depletion disturbance in 630.0 nm intensity (or plasma bubble signature) recorded on three photometers at Kolhapur at one minute interval at three zenith angles (30°E, 30°N and Zenith) on the night of 5 Mar. 1997. It was a spread-F night and the OI 630.0 nm emission shows strong periodic fluctuations in intensity at three zenith angles. There is wave propagation in all three directions. Figure 6 shows the power spectra of the three simultaneous

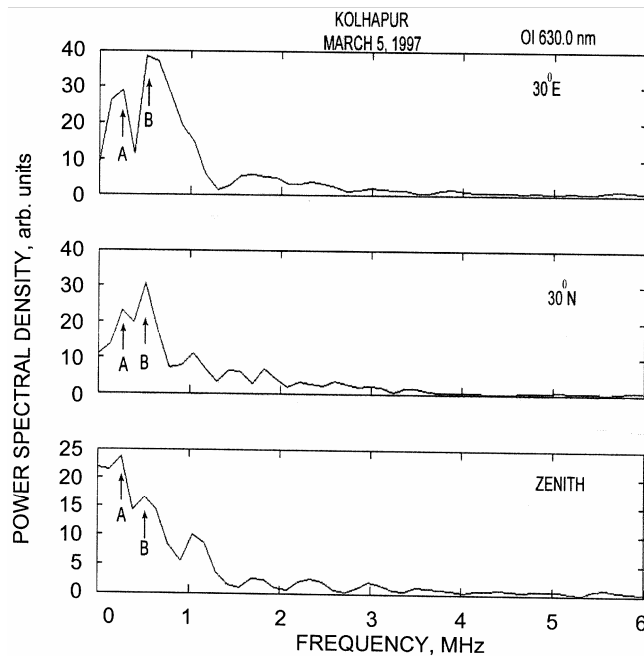


Fig. 6 — Power spectral density estimate of the three channel OI 630.0 nm intensity variation as a function of frequency (mHz) on the night of 5 Mar. 1997 at Kolhapur

data series of the OI 630.0 nm intensities on a Spread-F night as a function of frequency (mHz) after taking FFT with 256 points. It is clear from Fig. 6 that there is decrease in spectral power in OI 630.0 nm up to one mHz frequency peaking around 0.33 and 0.50 mHz marked by 'A' and 'B' in all the three zenith angles. They are the dominant frequencies with wave periods of about 50 and 33 min, present in the three sets of data series.

The depletions in OI 630.0 nm nightglow were observed from Brazil at 12°S geomagnetic latitude and also simultaneously in the OI 630.0 nm and OI 777.4 nm nightglow from the same latitude^{17,18}. Carman¹⁹ also reported the OI 630.0 nm depletions from Vanimo and compared them with common properties of equatorial plasma bubbles, such as depletion magnitude, cross-sectional size, and east-west drift, and found them to be in good agreement. The present findings are consistent with the earlier reported low latitude measurements of depletions from Brazil¹⁷, Ascension Island⁵ and India²⁰. The regions of decreased OI 630.0 nm intensity were north-south aligned, had east-west dimensions of 50-200 km, often extending to more than 1200 km in the north-south direction. The depletions appeared after sunset and were observed to drift to the east with 50-150 m/s. The present airglow depletions seem to move with the background plasma with similar

velocities to those previously reported by Yeh *et al.*²¹ They found an almost 150 m/s eastward drift with their plasma bubbles.

The seasonal variation of spread-F in the Indian longitude zone was reported by Subbarao and Krishnamurthy⁹. Statistical studies based on published data of f_oF2 from Trivandrum have revealed that equatorial spread-F depends inversely on magnetic activity during sunspot maximum period, but tends to disappear or even becomes positive in some seasons during the sunspot minimum period^{1,2,6,7,22}. Using the electron (e-h profile) density (N_A and N_W) data of Ahmedabad (dip latitude 18.6°N) and Waltair (dip latitude 10.6°N) in the Indian longitude zone, it was observed by Raghavarao *et al.*²³ that there was an enhancement in the electron density ratio (N_A / N_W) by a factor of 8-30 between the two stations around local evening hours compared to their day time values (N_A / N_W) on spread-F days. This was an intensification of northern crest of equatorial ionization anomaly situated near Ahmedabad during spread-F nights. No such enhancement was seen in electron density ratio (N_A / N_W) on nights without spread-F. The plumes observed by Woodman and La Hoz²⁴ move with background plasma velocity. Anderson and Mendillo²⁵ showed that in the absence of significant contribution from E-region horizontal current flows and tidally driven polarized electric fields, the equatorial zonal nighttime plasma drifts is given by

$$V_E = \frac{\int \sigma_p U B ds}{B \int \sigma_p ds}$$

where σ_p is the Pederson conductivity, U the zonal component of wind velocity and B the magnetic field intensity. The integrations are performed from one end of the field line in the northern hemisphere to the other end in the southern hemisphere. It is seen that the height profile of the flux tube integrated Pederson Conductivity can significantly affect the amplitude and altitudinal variation of the zonal plasma drifts.

On the basis of theoretical considerations it is suggested that nighttime plasma drifts near the equator are approximately equal to F-region neutral wind⁸. Therefore, with this consideration, the zonal and meridional components of equatorial plasma drift velocity are compared with the zonal and meridional components of neutral wind velocity computed from a model.

4 Comparison of observed plasma drift velocities with HWM model

In order to compare the observed plasma drift velocities, the Zonal component of neutral wind has been calculated during the period of observation. For this, the Hedin's empirical HWM 93 model⁷ has been used. This model is an extended version of HWM 90 model with variations in magnetic activity (Ap) included. Mid- and low-latitude data are reproduced quite well by the model. The model describes the transition from predominately diurnal variations in the upper thermosphere to semi-diurnal variations in the lower thermosphere and a transition from summer to winter flow above 140 km to winter to summer flow below 140 km. Significant altitude gradients in the wind extend up to 300 km at some local times. This model provides comprehensive statistical estimates based entirely on observational data. Inputs to the model include day of the year, local time, latitude, longitude, altitude, solar flux (F10.7 cm) and geomagnetic activity (Ap). The model software provides zonal and meridional winds for specified latitude, longitude, time, and Ap index.

In Table 2 the observed velocities to model predictions are compared. It also shows the ratio of the observed values to their model values. As may be seen, satisfactory agreement with the observations is obtained on most nights. However the observed meridional component at 2300 hrs IST on 18-19 Feb. 1993 is much higher than the model predicted value. This could be due to lack of sufficient data coverage in the low latitude region of the thermosphere used to calculate model coefficients and also, local features are not included in the average model.

Thus, this comparison of the zonal plasma drift speed with theoretical zonal neutral wind velocity measurements from HWM 93 model shows the fact that in general the nighttime zonal component of the neutral wind and the ambient plasma move in the same direction with nearly equal velocities.

5 Behaviour of thermospheric winds (zonal and meridional) from theoretical calculations

To observe the variability of the thermospheric winds with time and altitude, the meridional and zonal component of the neutral wind have been calculated at several heights (300-650 km) using HWM93 model⁷ for 18-19 Feb. 1991 at Kolhapur with appropriate geophysical parameters. In Fig. 7 the variation of the two components of the wind velocity is shown as a function altitude from 300 to 650 km at an interval of 50 km. The plots show that the zonal component changes its direction near the sunset and after the sunset it enhances suddenly to larger values, with peak in velocity at 2000-2100 hrs IST. This is due to the so called pre-reversal enhancement, which is the one of the conditions for the onset of Spread-F.

The meridional component of the neutral wind is also calculated using the HWM93 model (Fig. 7) and the results show that the meridional wind velocity decreases after midday and it changes its sign near sunset. In the day time the meridional wind blows pole ward and in the night time it blows equator ward, which is the main cause that affects the F-region height. When the meridional wind blows pole ward, the wind pushes down the F-layer and when it goes equator ward, it lifts the F-layer upwards, which is the one of the causes of the persistence of the nighttime F-layer. So, in the nighttime due to meridional wind the F-layer goes up, which prevents it from collapse due to recombination. From Fig. 7, it is observed that the direction of the wind changes at 2030 hrs IST and as time goes on velocity further reduces with a minimum at 2300 hrs IST of 10 m/s in that direction. After that the velocity surges again and changes its sign before sunrise. There is also increase in wind velocity as a function of height around local noon hours.

To know the latitudinal variation of the zonal component of the neutral wind, the zonal and meridional components of the neutral wind velocities have been calculated for various low latitude stations,

Table 2 — Comparison of observed velocities to their model predicted values

Date	Time, hrs IST	Observed velocity, m/s	Velocity computed from HWM93 model, m/s	Ratio of observed/model velocities
18-19Feb.1991	0045-0140	150 (W-E)	152	0.99
20-21 Feb.1991	2245	130 (W-E)	106	1.23
21-22 Feb.1993	2200	152 (N-S)	153	0.99
18-19 Feb.1993	2300	175 (N-S)	70	> 1
	0300	175 (N-S)	33	> 1

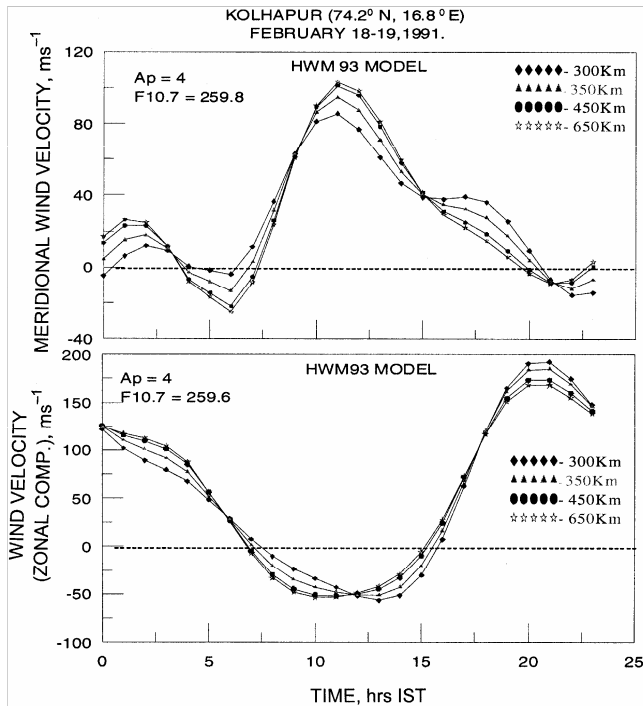


Fig. 7 — The meridional and zonal components of neutral wind velocity computed at 300, 350, 450 and 650 km altitudes on 18-19 Feb. 1991 at Kolhapur using HWM93 model

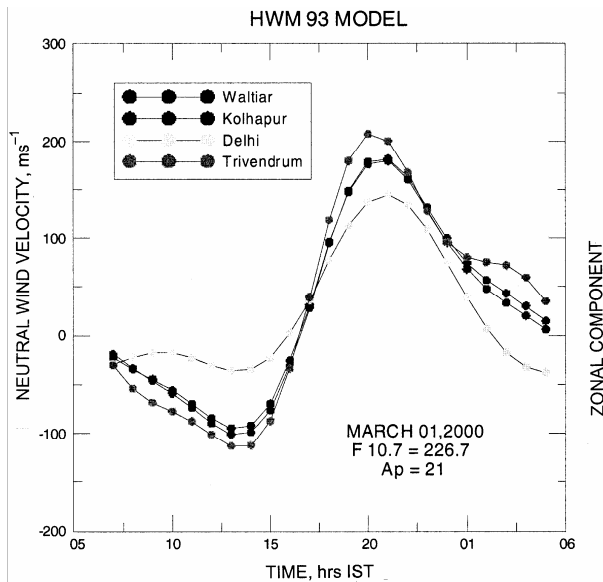


Fig. 8 — Zonal wind velocities from HWM model for the station Trivandrum, Visakhapatnam, Kolhapur and Delhi on 1-2 Mar. 2000

Trivandrum (8.2°N, 76.9°E, dip latitude 0.3°N), Waltair (17.7°N, 83.3°E, dip latitude 20°N), Kolhapur (16.8°N, 74.2°E, dip latitude 10.6°N) and Delhi (28.6°N, 77.2°E, dip latitude 33°N) using HWM 93 model. The plots for the calculated values are shown in Fig. 8. The maximum velocities of the zonal

component peak are obtained for all the stations around 2000-2100 hrs IST. It shows that the zonal winds depend on the latitude and is larger at the equator, decreases in magnitude as one moves away from the equator. The zonal wind velocities are seen to be higher for the Trivandrum station, which is nearer the equator and low for Delhi station, which is far away from the equator than other stations. According to Anderson *et al.*²⁶, the latitude dependence of the zonal wind component is $U = U_{eq} \cos(4\Phi)$, where Φ is dip angle and U_{eq} is the velocity of the wind at the dip equator. The present calculations also confirm the above empirical relationship.

6 Conclusions

Simultaneous observation of thermospheric OI 630.0 nm nightglow at a low latitude station, Kolhapur has been presented, using three tilting filter photometers linking the observations to the process of low latitude Spread-F phenomena and the movement of plasma depletions. The principal findings of the present investigation are summarized below:

(a) The meridional and zonal motions of the thermosphere computed from the model compares well with the observations, establishing the fact that neutral wind velocities and plasma move with the same speed at night. This confirms the suggestion that the observed zonal plasma bubble drift velocities and the zonal neutral wind velocities (HWM-93 model) near the equator are approximately equal to the F-region neutral winds²⁷. The zonal F-region wind dynamo drives the Pederson currents and creates a vertical polarization electric field, which forces the plasma to drift at nearly the same velocity as the neutral wind velocity²⁸⁻³². The large discrepancies between the values on 18-19 Feb. 1993 could be due to insufficient data coverage at Indian low latitude stations to get the coefficients of the model.

(b) As given by the HWM model, the zonal winds peak at the equator around 2030 hrs IST. The local time variations of the zonal wind computed from the model match well with the equatorial zonal neutral wind as measured by the WATS instrument on the DE-2 satellite in 1981 and the zonal ion-drift as measured from the ground with the Jicamarca incoherent scatter radar⁶.

(c) Spectral analysis of the three components of OI 630.0 nm intensity variation during a spread-F night (5 Mar. 1997) yields the dominant periodicities in the range of 33-50 min, which could be the typical wave

periods of the gravity waves that produce the perturbation electric fields, thereby causing the growth of the plumes in the equatorial Spread-F.

Acknowledgements

The nightglow observations at Kolhapur were carried under collaborative research program between IIG, Navi Mumbai and Shivaji University, Kolhapur. Technical support received from Mr P T Patil in Airglow work is gratefully acknowledged. The authors are grateful to the two referees for their valuable comments to improve the quality of the paper.

References

- Mukherjee G K, Studies of equatorial F-region plasma depletions and dynamics using multiple wavelength nightglow imaging, *J Atmos Sol-Terr Phys (UK)*, 65 (2003) 379.
- Weber E J, Buchau J, Eather R H & Mende S B, North-south aligned equatorial airglow depletions, *J Geophys Res (USA)*, 83 (1978) 712.
- Mukherjee G K & Dyson P L, A filter tilting photometer for nightglow measurements of 630.0 nm emission line, *Indian J Radio Space Phys*, 92 (1992) 212.
- Rastogi R G & Aaron J, Night time ionospheric radio scintillations and vertical drifts at the magnetic equator, *J Atmos Terr Phys (UK)*, 42 (1980) 583.
- Mendillo M & Baumgardner J, Airglow characteristics of equatorial plasma depletions, *J Geophys Res (USA)*, 87 (1982) 7641.
- Hysell D L Kelley M C Swartz W E & Woodman R F, Seeding and layering of equatorial Spread-F by gravity waves, *J Geophys Res (USA)*, 95 (1990) 17253.
- Hedin A E, Fleming E L, Mansion A H, Tsuda T, Vial F & Vincent R A, Empirical wind model for the upper, lower and middle atmosphere. *J Atmos Sol-Terr Phys (USA)*, 58 (1996) 1421.
- Herrero F A, Spencer N W & Mayr H G, Thermosphere and F-region plasma dynamics in the equatorial region, *Adv Space Res (UK)*, 13 (1993) 201.
- Subbarao K S V & Krishnamurthy B V, Seasonal variations of equatorial spread-F, *Ann Geophys (France)*, 12 (1974) 1.
- Sobral J H A & Abdu M A, Latitudinal gradient in the plasma bubble zonal velocities as observed by scanning 630-nm airglow measurements, *J Geophys Res (USA)*, 95 (1990) 8253.
- Thomson D J, Spectrum estimation and Harmonic analysis, *Proc of IEEE (USA)*, 70 (1982) 1097.
- Dyson P L & Hoggood P A, The interpretation of 6300 Å airglow observations of ionospheric irregularities, *Planet Space Sci (UK)*, 22 (1974) 495.
- Rishbeth H, Gordon R, Riss D & Fuller-Rowell T J, Modelling of thermospheric composition changes caused by a severe magnetic storm, *Planet Space Sci (UK)*, 33 (1985) 1283.
- Takahashi T, Oya H & Watanabe S, Ionospheric disturbances induced by storm associated electric fields in the low latitude F-region, *J Geomag Geoelect (Japan)*, 39 (1987) 187.
- Fesen C G, Crowley G & Roble R G, Ionospheric effects at low latitudes during March 22, 1979, Geomagnetic storm, *J Geophys Res (USA)*, 94 (1989) 5405.
- Sahai, Y, Bitteencourt J A, Takahashi H, Teixeira N R, Tinsley B A & Rohrbaugh R P, Analysis of storm-time low latitude simultaneous ionosphere and nightglow emission measurements, *J Atmos Terr Phys (UK)*, 52 (1990) 749.
- Sobral J H A, M A Abdu & Sahai Y, Equatorial plasma bubble eastward velocity characteristics from scanning airglow photometer measurements from Cachoeira Paulista, *J Atmos Terr Phys (UK)*, 47 (1985) 895.
- Mukherjee G K, Parihar Navin, Niranjana K & Manju G, Signature of Midnight Temperature Maximum (MTM) using OI 630 nm Airglow, *Indian J Radio Space Phys*, 35 (2006) 14.
- Carman E H, Equatorial depletions in 630.0 nm airglow at VANIMO, *Planet Space Sci (UK)*, 31 (1983) 355.
- Sinha H S S, Mishra R N, Chandra H, Shikha Raizada, Dutta N & Vyas G D, Multi-wavelength optical imaging of ionospheric plasma depletions, *Indian J Radio Space Phys*, 25 (1996) 44.
- Yeh K C, Soicher H & Liu C H, Observations of equatorial ionospheric bubbles by the radio propagation method, *J Geophys Res (USA)*, 84 (1979) 6589.
- Somayajulu V V & Krishnamurthy B V, The nature of association of equatorial spread-F with magnetic activity, *Nature (UK)*, 263 (1976) 36.
- Raghava Rao R, Sastri Hanumath, Vyas G D & Sriramrao M, Role of equatorial ionization anomaly in the initiation of equatorial spread-F, *J Geophys Res (USA)*, 93 (1988) 5959.
- Woodman, R F & La Hoz C, Radar observations of F-region equatorial irregularities, *J Geophys Res (USA)*, 81 (1976) 5447.
- Anderson D N & Mendillo M, Ionospheric conditions affecting the evolution of equatorial plasma depletions, *Geophys Res Lett (USA)*, 10 (1983) 541.
- Anderson D N, Heelis R A, and McClure J P, Calculated nighttime eastward plasma drift velocities at low-latitudes and their solar cycle dependence, *Ann Geophys (France)*, 5A (1987) 35.
- Biondi M A, Meriwether Jr J W, Fejer B & Woodman R, Measurements of the dynamics and coupling of the equatorial thermosphere and F region ionosphere over Peru, *J Atmos Terr Phys (UK)*, 45 (1988) 697.
- Rishbeth H, The F-layer dynamo, *Planet Space Sci (UK)*, 19 (1971) 263.
- Mitra S N, Horizontal motion in ionospheric regions-A review, *Indian J Radio Space Phys*, 15 (1986) 295.
- Sreehari C V, Bhuvandrawn C & Prabhakaran Nayar S R, HF Doppler radar observations of vertical and zonal plasma drifts –signature of plasma velocity vortex in the F-region, *Indian J Radio Space Phys*, 35 (2006) 242.
- Oyekola O S, Akinremi Ojo & Akinrimisi Jolasun, *Indian J Radio Space Phys*, 35 (2006) 227.
- Jayachandran P T, Sriram P, Somayajulu V V & Rama Rao P V S, Effect of equatorial ionization anomaly on the occurrence of Spread-F, *Ann Geophys (France)*, 15 (1997) 255.